Achilles Stiffness & Weakened Calf Muscles

Exoskeleton Design

DIVIK BHARGAVA, NAREK DIVANYAN, LOGAN HALL, PRUTHAK JOSHI, PHILIP NG

I. Introduction

The Achilles tendon is the largest and strongest tendon in the body, connecting the calf muscles to the heel bone. Achilles tendon pathology encompasses a range of conditions affecting the Achilles tendon. One common pathology is Achilles tendon stiffness, characterized by reduced flexibility and mobility in the tendon. This stiffness can significantly impact gait mechanics, as the Achilles tendon plays a crucial role in ankle movement during walking, running, and jumping. Various factors contribute to Achilles tendon stiffness, including overuse or repetitive stress from activities like running or jumping, muscle imbalances such as weakness or tightness in the calf muscles, and previous injuries or aging.

The stiffness of the Achilles tendon can lead to muscle weakness in the calf muscles, particularly the gastrocnemius and soleus muscles, due to altered biomechanics and reduced ability to generate force effectively. This muscle weakness can further exacerbate gait abnormalities, such as reduced push-off power during walking, altered heel strike, and compensatory movements in other joints to accommodate for the decreased mobility and strength in the affected leg. Complications in gait caused by Achilles tendon stiffness may include a shuffling gait pattern, reduced stride length, and increased risk of falls due to impaired balance and stability. Overall, Achilles tendon pathology can have significant implications for gait mechanics, leading to muscle weakness, altered movement patterns, and increased risk of musculoskeletal issues, underscoring the importance of replicating its function and restoring mobility by means of a Bionic device. Current treatment methods include using Ankle-Foot Orthoses, braces, splints, physiotherapy, and self-care.

II. Biomechanical Modeling

a. Stiffened Archilles tendon can cause pain and discomfort during walking. This pathology also affects tendon stiffness, which can be modeled by changing the slack length in OpenSim. Often, Archilles tendon is associated with weakened calf muscles, which will be enforced in OpenSim by changing the maximum isometric force of the SOL and GAS muscles. Through biomechanical modeling, we aim to propose a bionic system which can supplement plantarflexion, reducing the force requirement for GAS and SO, in turn taking off load from the stiffened tendon. The bionic system will supplement plantarflexion, reducing the force requirement for Gastro and Soleus in turn taking off load from stiffened tendon.

b. To model the pathology in OpenSim, we reduced the tendon slack length and the maximum isometric force of the Gastrocnemius and Soleus muscles to simulate the stiffened Achilles tendon. We maintained the same gait of the model, while changing the muscle properties, to analyze the effect of the muscle properties on the metabolic costs of the GAS and SOL muscles. We expect higher metabolic costs with added pathology than healthy muscles, which is also observed with the metabolic cost generated by OpenSim (Fig. 3 and 4). To choose the slack length and isometric force that closely replicate the pathology, we calculated the metabolic costs associated with 24 different combinations of tendon slack length and max isometric force. These results helped us understand how the metabolic cost varies with changing slack length and isometric force.

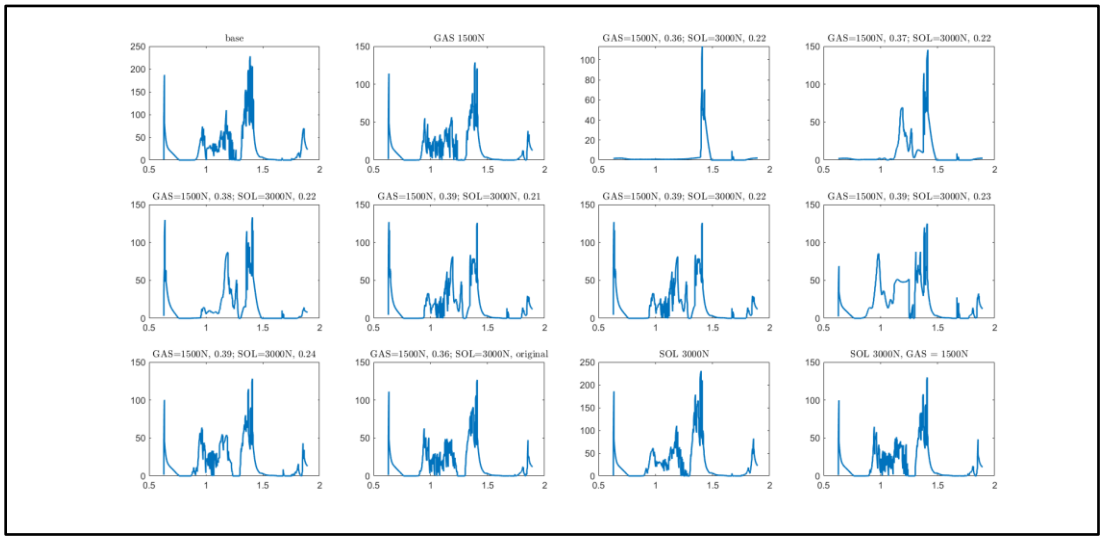

Fig. 1: Metabolic cost of GAS muscle with varying the total isometric force and the tendon slack lengths of GAS and SOL

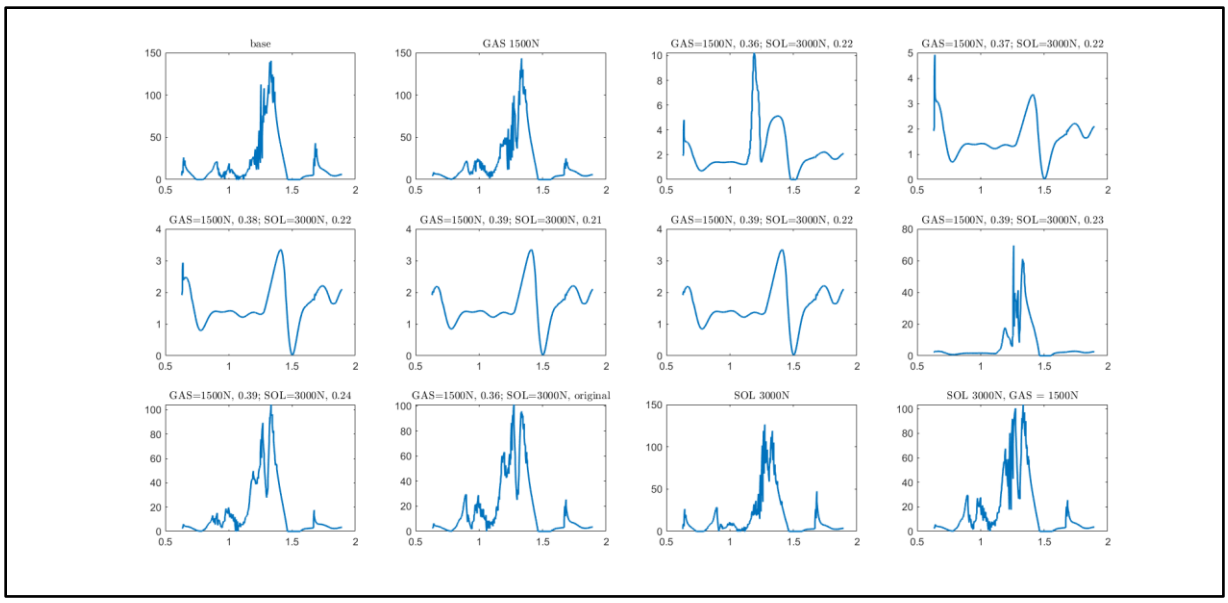

Fig. 2: Metabolic cost of SOL muscle with varying the total isometric force and the tendon slack lengths of GAS and SOL

c. Based on the results in Fig 1 and Fig 2, we down selected the following parameters for our model in OpenSim.

	Tendon Slack Length		**Maximum Isometric Force**	
	Healthy	With Pathology	Healthy	With Pathology
GAS	0.39m	0.38m	2500N	1300N
SOL	0.2514m	0.24m	5137N	3000N

Table 1: OpenSim Parameter Selection

d. Metabolic cost Comparison

With these finalized parameters, we generated the GAS, SOL, and total metabolic plots (Fig. 3 and 4). As expected, the pathology increases the metabolic cost of the gait, which is more pronounced at the plantarflexion phase of the gait, where the muscles are incapable of producing sufficient force during lift off. Through our bionic system design, we aim to bring the metabolic cost down to the metabolic cost of a healthy body through supporting plantarflexion motion.

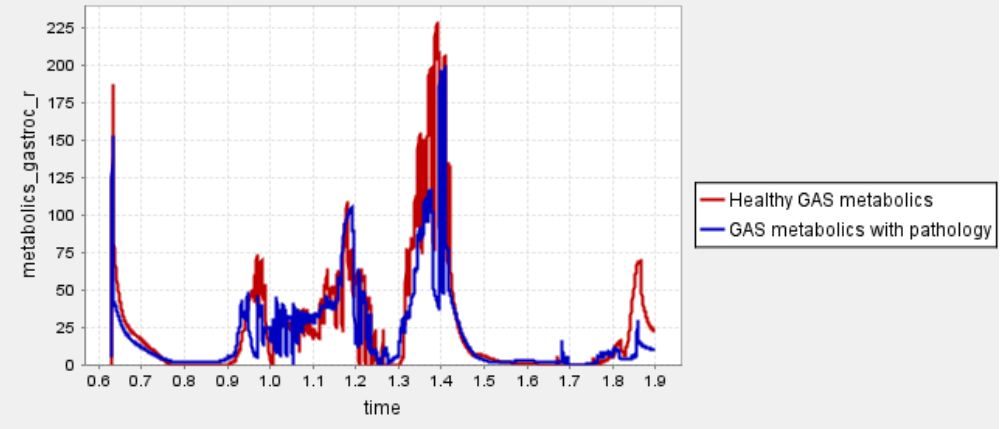

Fig. 3: Metabolic cost of GAS muscle with finalized pathology parameters

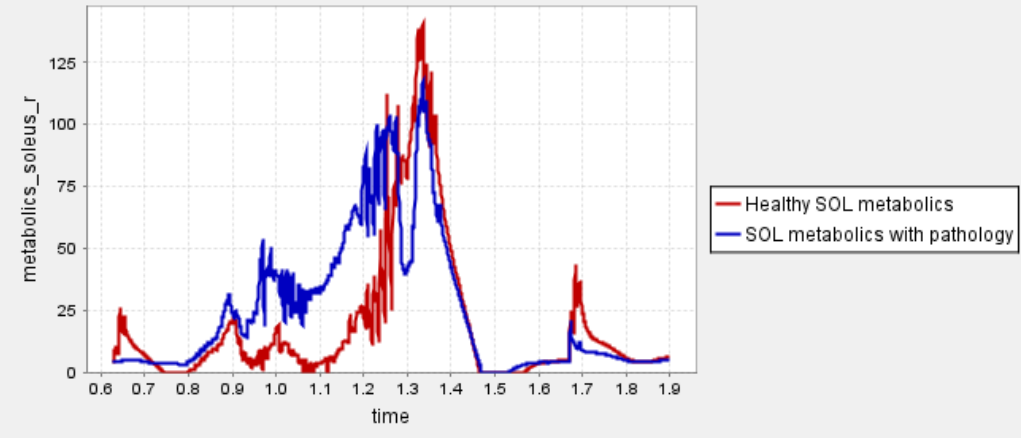

Fig. 4: Metabolic cost of SOL muscle with finalized pathology parameters

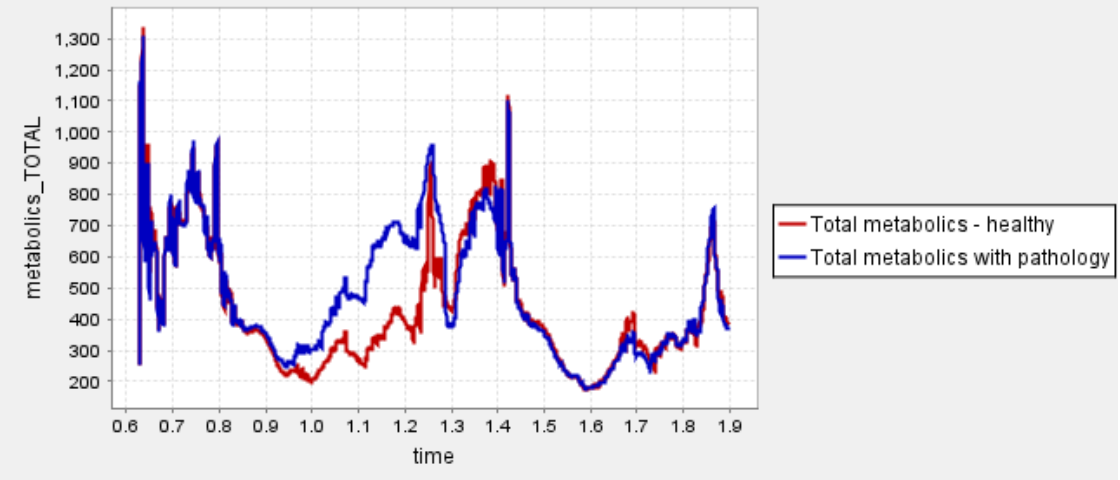

Fig. 5: Total metabolic cost with finalized pathology parameters

e. Modeling Path Actuator

To support the plantarflexion and reduce force exerted by calf muscles, we modelled a Path Actuator in OpenSim. The path actuator placement and maximum isometric force is optimized to reduce the GAS and SOL force and distribute the force more evenly between the two muscles and the actuator. We ran CMC for different actuator placement and properties and calculated the force profiles as below.

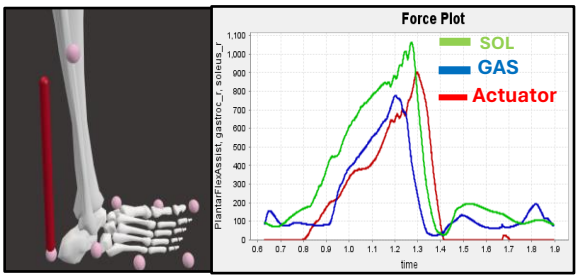

Iteration 1: Optimal Force 1500N, L_H=6cm

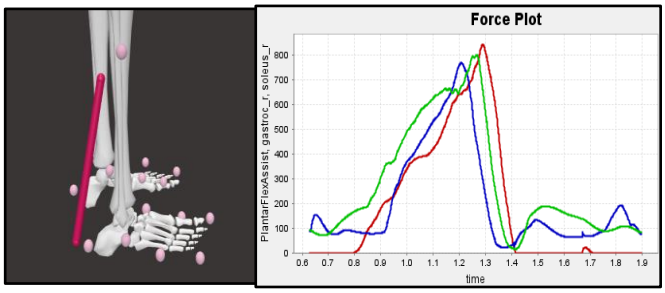

Iteration 2: Optimal Force 1500N, L_H=8.5cm

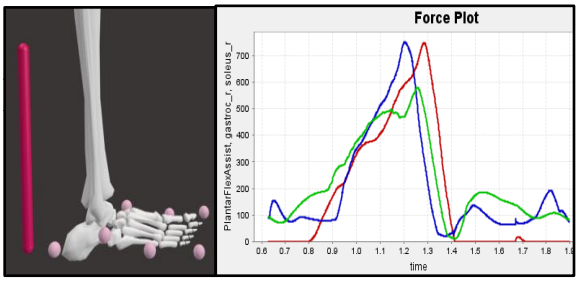

Iteration 3 - Optimal Force 1500N, L_H = 10cm

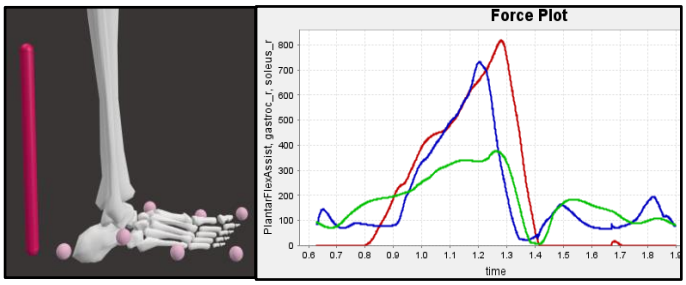

Final Design - Optimal Force 2000N, L_H = 10cm

Fig. 6: Path Actuator Optimization

When the actuator is placed close to the heel, the moment produced is less for a given force the actuator. This leads to increased force requirement of the muscles, especially Soleus. As the L_h is increased, the moment arm of the actuator increases, which increases the plantarflexion moment by the actuator. Therefore, for the first three iterations, we tried to increase the moment arm while keeping the maximum force of the actuator as 1500N. As seen from the force plots, the SOL and actuator force decreases, with increases moment arm but not substantially. Upon increasing the optimal force to 2000N, we force the actuator to produce more force thereby further reducing the Soleus muscle force. Thus, we optimized the actuator placement and its force in OpenSim to yield maximum force reduction of the muscles and optimize the force distribution between the muscles.

f. Residual Analysis

The residual analysis shows the moment has high fidelity, and the capable of producing acceptable results.

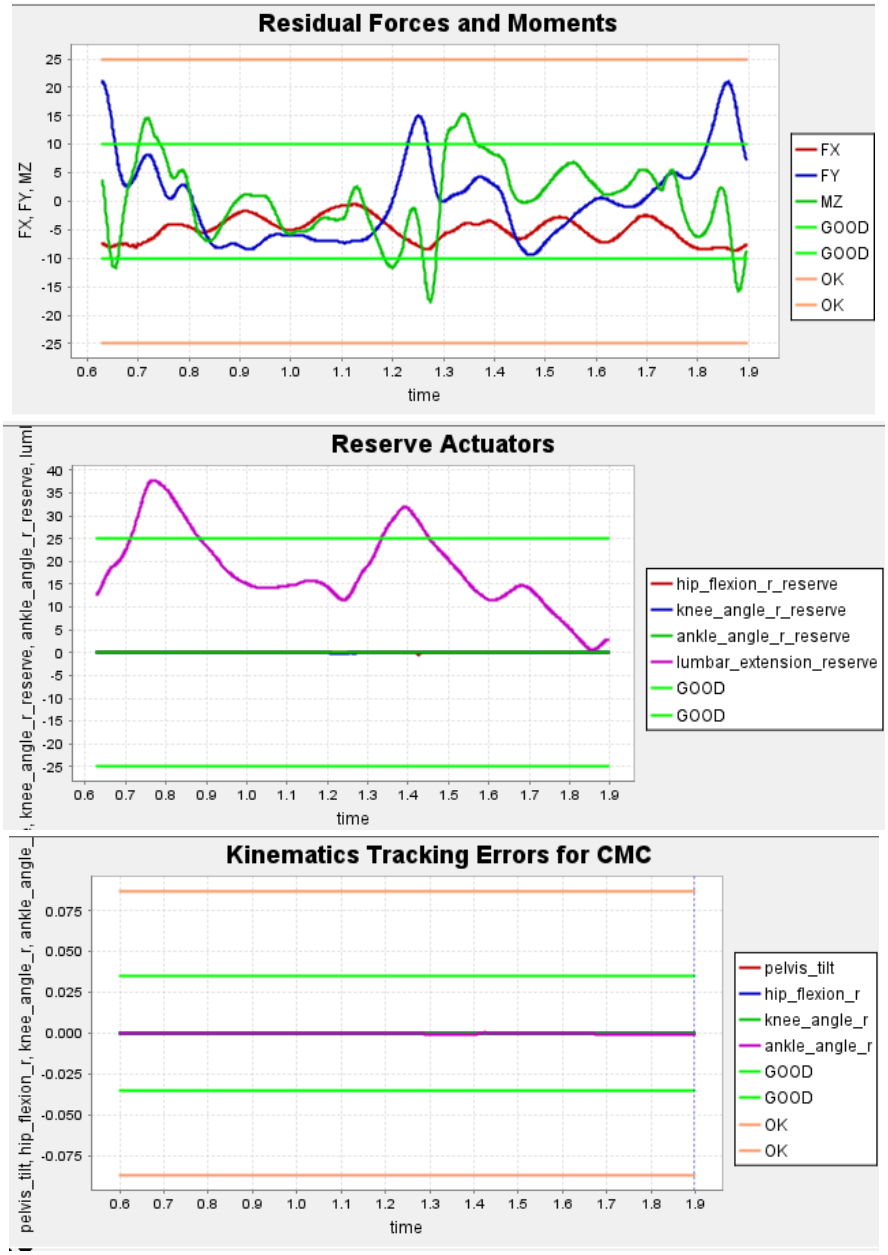

Fig. 7: Residuals Plots

g. Performance Comparison

Using an assistive bionic device, we were able to reduce the peak force requirement of Soles muscle by 82% of its original value. By reducing the force applied by the muscle we reduce the stretch and discomfort due to the stiffened tendon. Refer Figure 8a.

Subsequent analysis in the later section yields the mass of the bionic system to be 4kg along with all the electronics, motor, battery, and enclosure. To perform a realistic performance comparison, we applied a mass of 4kg on the tibia bone in OpenSim and compared the metabolic cost comparison. Integral of metabolic cost comparison shows that adding bionic device does not increase metabolic cost compared to pathology. However, there is significant potential to reduce the metabolic cost by reducing the overall weight of the system by choosing a lighter custom battery. Figure 8b shows the metabolic cost comparison, and we can see that adding a bionic device does not add to additional metabolic cost.

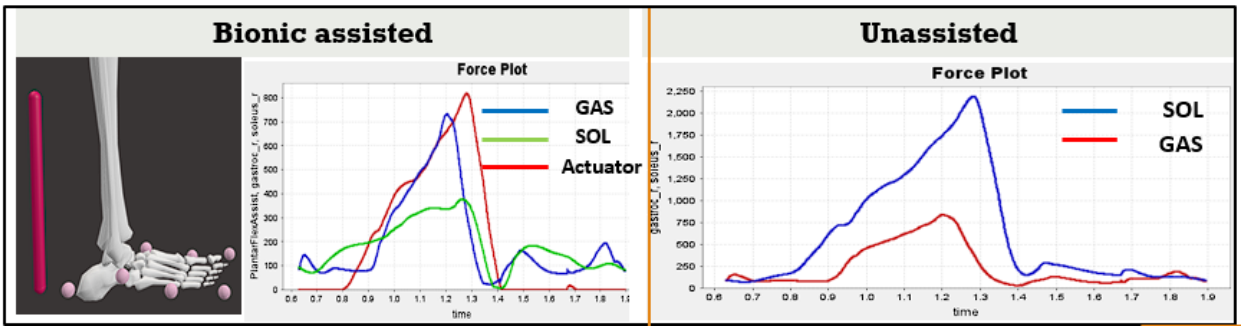

Figure 8a: Force comparison.

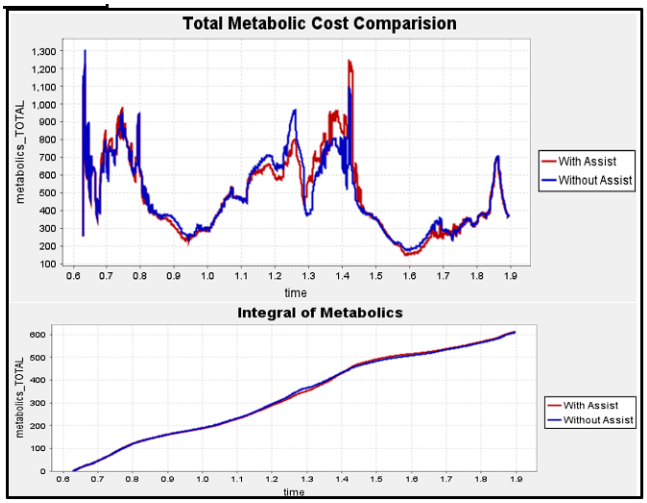

Figure 8b: Metabolic cost Comparison.

III. Bionic System Design

a. Motor Selection & Transmission Ratio Optimization

Once we optimized the actuator parameters (force and placement) in OpenSim, we computed the actuator moment arm variation with time using a python script in OpenSim. With both force and moment arm data, we then computed the moment at the ankle coordinate, which is then used to inform the motor selection for our system (Fig 9a).

To start our motor selection, we identified six potential candidates, as described in Table 2. To decide on one of these motors, we ran a brute force optimization, comparing each motor's average power lost due to heat over a range of transmission ratios from N = 10 to N = 1000. From the plot shown in figure 9, we then selected motor 3 and identified a target transmission ratio between 100-130.

Params	Motor 1	Motor 2	Motor 3	Motor 4	Motor5	Motor 6
Name	Maxon EC Max Ø40mm	Maxon DCX 35 Ø35mm	U8-KV100 Ø87mm	Maxon DCX 35 Ø35mm	Maxon DCX 32 Ø32mm	Maxon A max Ø26 mm
Terminal R	4.4 Ω	1.76 Ω	0.186 Ω	0.716 Ω	1.42 Ω	70.2 Ω
Terminal L	0.937 mH	0.658 mH	0.138 mH	0.26 mH	0.473 mH	6.68 mH
Torque cons	96.1 mNm/A	68.3 mNm/A	140 mNm/A	42.9 mNm/A	58.5 mNm/A	75.2 mNm/A
Inertia	101 gcm²	99.5 gcm²	1200 gcm²	98.7 gcm²	75.9 gcm²	12.1 gcm²
Weight	720g	385g	230g	385g	325g	117g

Table 2: Motor Selection

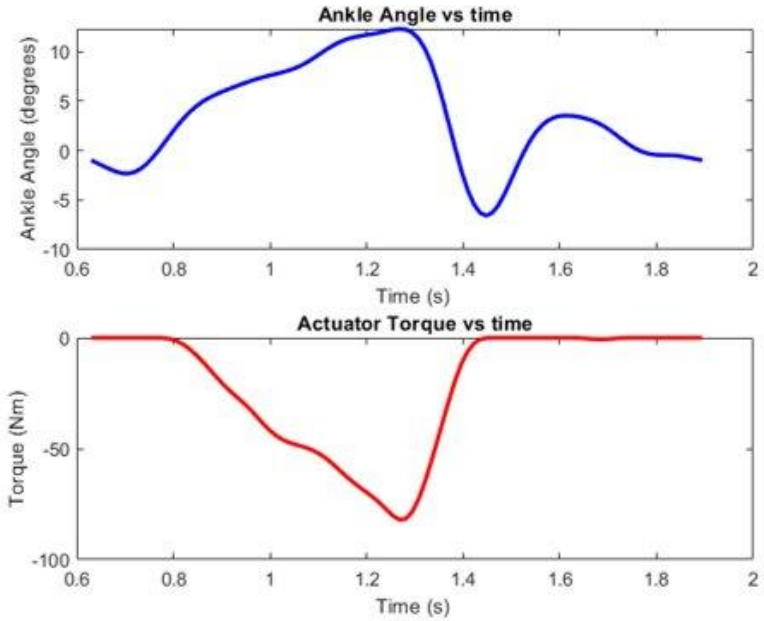

Fig. 9a: Ankle angle and torque vs time

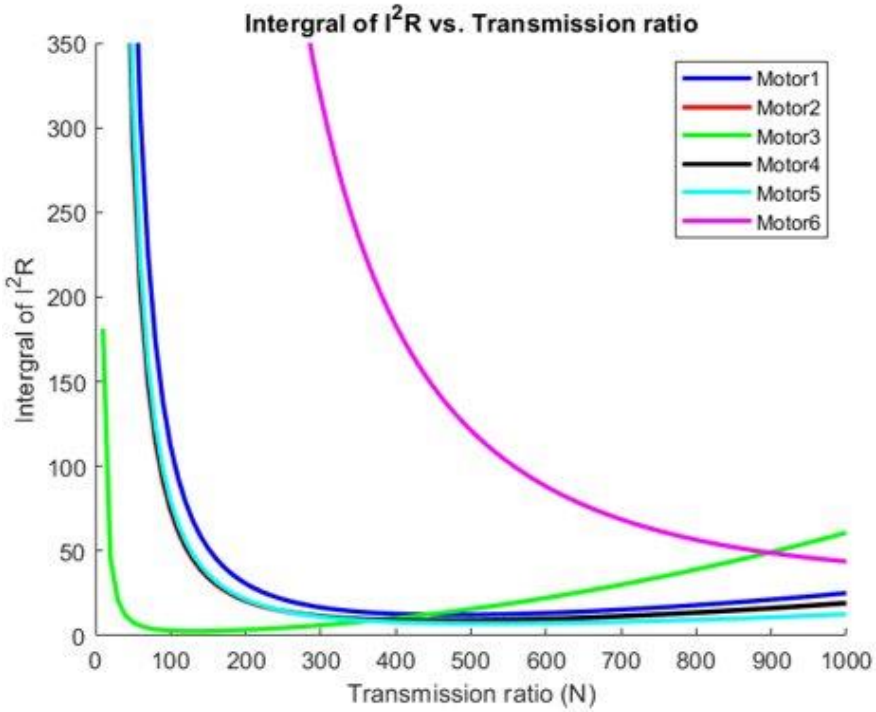

Fig. 9b: Motor selection – Transmission ratio vs average power lost to heat.

b. Adding SEA Spring

We propose adding a Serial Elastic Spring to provide a jerk free and efficient motion at the ankle during the plantarflexion. We ran a brute force optimization for spring stiffness(k) to yield the lowest power lost to heat at different transmission ratio N=80, N=100 and N=130.

We find that the spring stiffness between 150 – 180 Nm/rad is the most optimum in terms of power lost to heat at N=100 and voltage requirements. A spring stiffness with higher TR like N=130, although it is marginally more efficient, requires peak voltage greater than 48V, which will demand for a bulkier battery. Therefore, by choosing the K=180Nm/rad at N=100, we were able to keep the peak voltage requirement less than 48V.

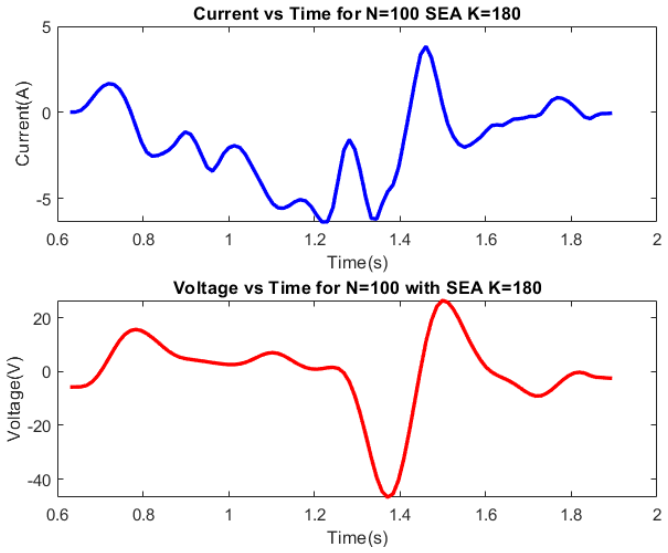

Fig. 10a: Current and Voltage requirement with SEA K=180NM/rad N=100

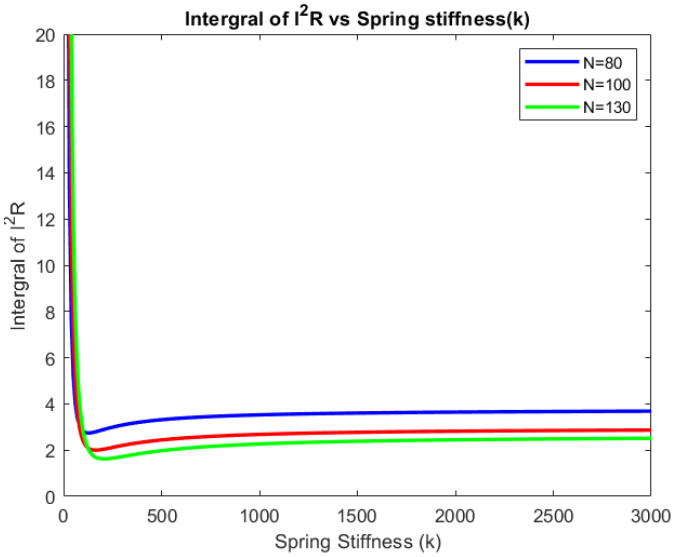

Fig. 10b: SEA Stiffness Optimization for average power lost to heat.

c. Battery Requirements

From the current and voltage requirements in Fig. 10a the total energy consumed by the system would be around 11.60Joules/gait. To achieve 5000 steps per day, we require a battery with capacity minimum 437mAh. Below is the candidate off the shelf battery with can provide a peak voltage of 54.6V, and max current 25amp rated at a capacity of 5000mAh. Using this battery, we can estimate the battery life of the prosthesis to be around 11 days.

d. Transmission Design

From motor selection, we have the target transmission ratio of N=100 to N=130. To achieve this, we designed a three-part transmission, consisting of a planetary gear, a rotary to linear transmission (represented by the spool), and a linear to rotary transmission (given by the modified ankle joint). This leads to a nonlinear transmission ratio, hence we are targeting the range of N = 100-130, instead of one discrete value. We selected a planetary gear with a 45:1 gear ratio and a spool with a 0.040m diameter. Our chosen parameters led to a transmission with a transmission ratio defined in figure 11 over a range of ankle angles. Examples of the gearbox, spool, and motor are shown in figure 12.

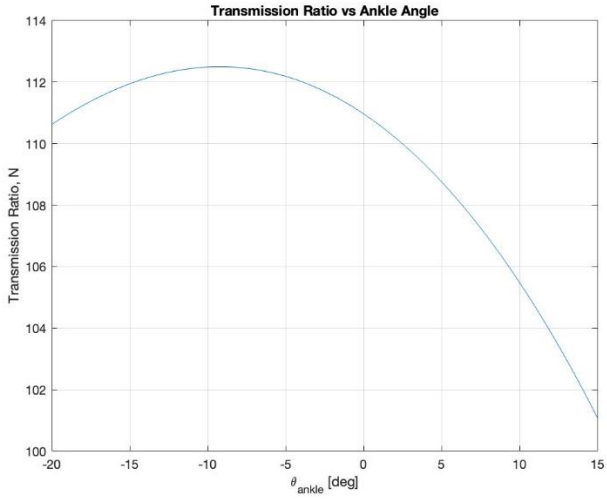

Figure 11: Transmission ratio vs Ankle angle

Figure 12: Examples of chosen planetary gearbox, spool, and motor.

e. Concept Design

Our concept design for this prosthesis is sketched in figure 13. The design allows the user to simply step into the device and strap the prosthesis to two places - their foot and lower leg. All the components were intentionally kept below the knee to minimize issues that would come from the added complexity of movement and actions such as sitting. The device works by having the motor actuate to spool up the lanyard/cord in plantarflexion, and then the device passively unreels with dorsiflexion. To mitigate the issues that are potentially caused by a cord-based system, our design incorporates a torsion spring (figure 13) that always keeps a light torsion on the spool to help it spool up. The motor placement was intentionally moved to attach close to the leg to minimize unnecessary complexity and moments on the system. Our cooling method (figure 14) consists of a custom machined aluminum collar to fit around the motor. The collar would then be sealed with an aluminum thermal paste to convectively dissipate the motor heat. Our resulting system has an estimated weight of 4.02 kg with a torque density of approximately 0.74 Nm/kg.

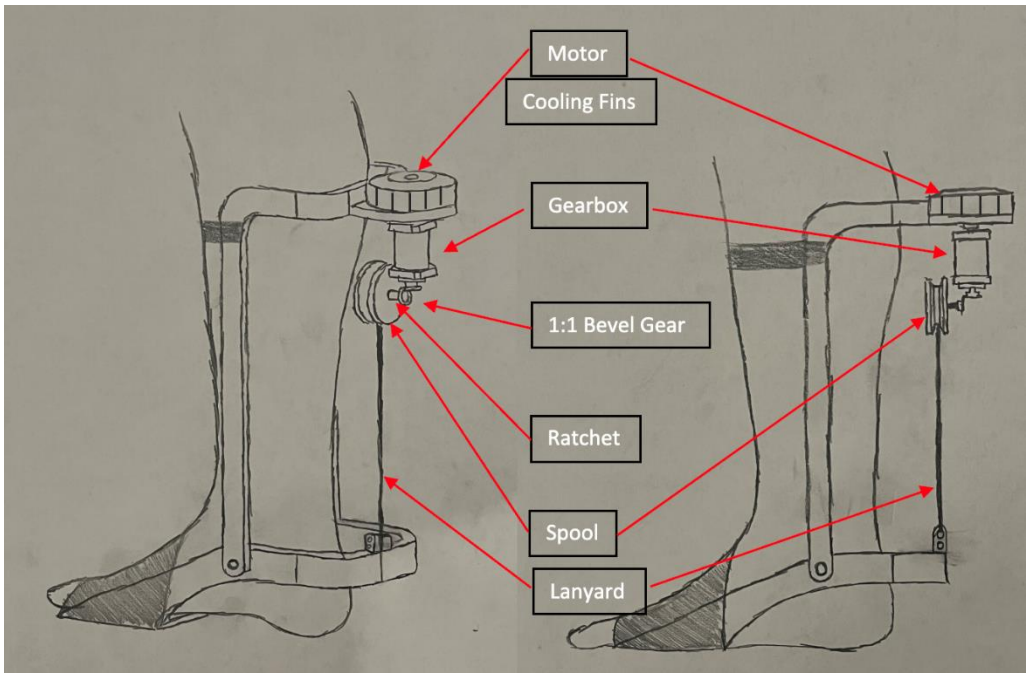

Fig. 13: Prosthesis Concept Design (Some Components Hidden for Clarity)

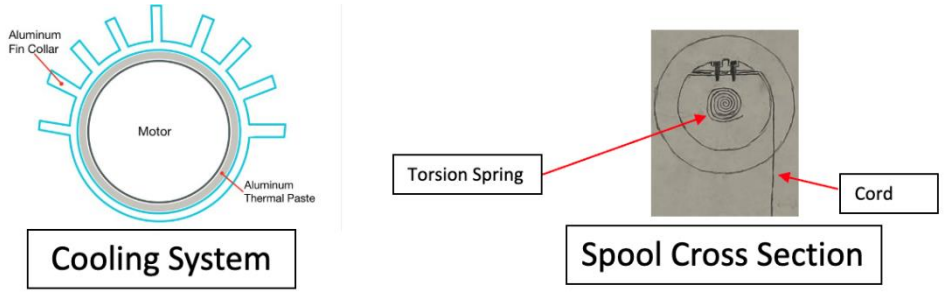

Fig. 14: Cooling System and Spool Details

IV. Controls and Comms

a. Low-Level, Mid-Level, and High-Level Design

At a high level, the goal of this bionic system is to make up for the lack of plantarflexion torque during gait. The system will receive EMG data to figure out the state/phase of gate that the user is in. From this the control system will output the desired ankle moment and angle, as received from the OpenSim results. Moving on to the low and mid-level design, the important joint dynamics that we need to know are the transmission ratio (N = 100) and the motor equation: $T_m = J_m \theta_m'' + b_m \theta_m' + T_L$. Then, we know the desired T_m , which is the motor reservoir torque. From here we need to determine how much current to deliver and how we are going to control the error performance signal.

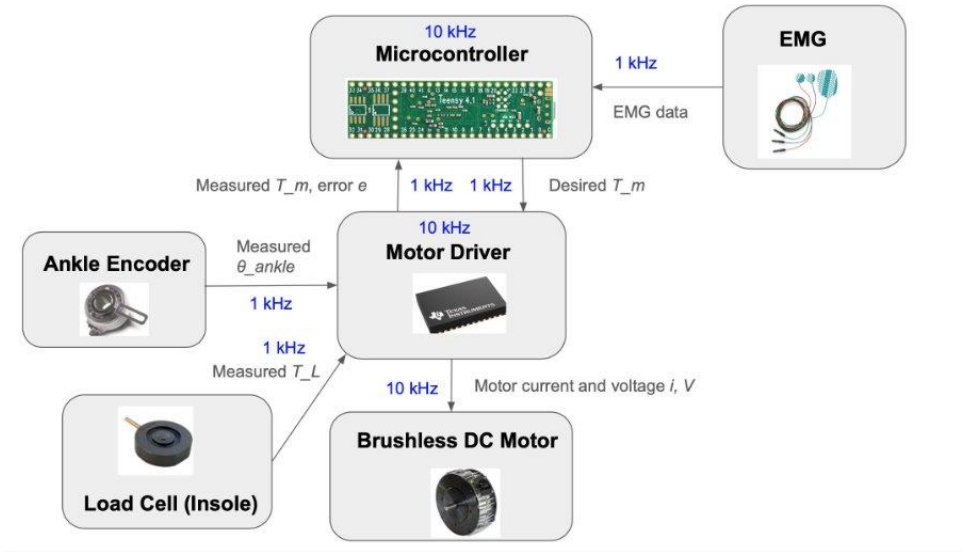

Fig. 15: Selected Control Hardware

b. PID Control

The Simulink model depicted in the Figure 16 and 17 represents a control system for the bionic system. The focus is on the motor and transmission dynamics. The input, labeled "Actuator Data," feeds into the system. The output includes two signals: θ_ankle (related to motor position) and T_mref (reference torque). A feedback loop calculates an error 'e' based on the difference between the reference and measured torque. The PID controller processes this error and adjusts the motor torque accordingly. The final output is the motor torque (T_m). Additionally, sensor noise is introduced to the sensor reading before error calculation. Overall, the model aims to regulate the motor torque using feedback control.

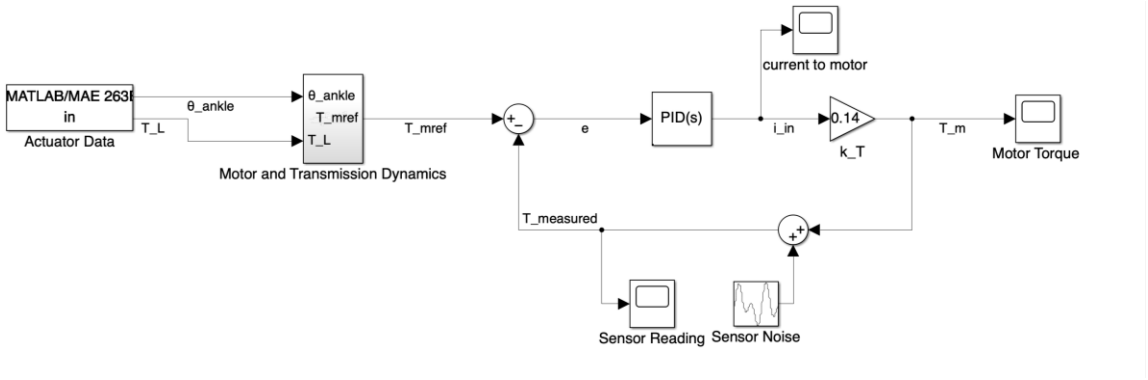

Fig. 16: Simulink calculation for motor torque

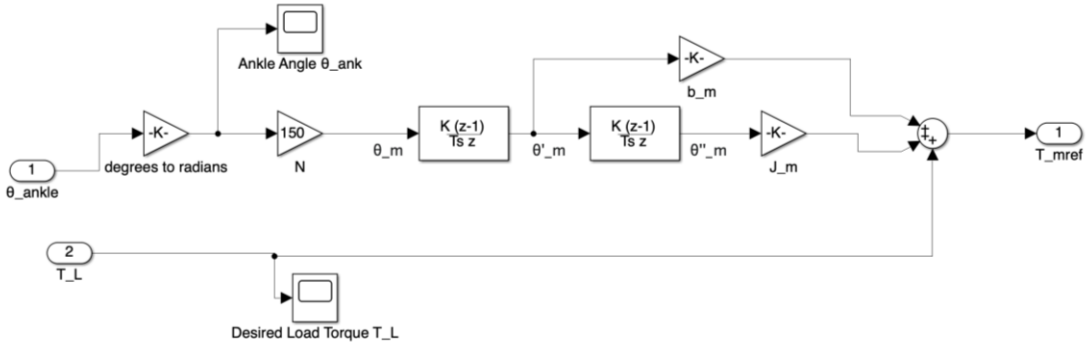

Fig 17: *Simulink* for reference torque

c. Coms / Control Hardware

Our selected control hardware is shown in figure 15. We chose a teensy 4.1 microcontroller, which has a low number of input/output channels needed, one I2C line and is C based code. For our motor driver, we selected the MCF8315C-Q1 brushless DC motor driver, which uses sensorless field oriented control (FOC). The rotary encoder we selected is the Turck Ri-43Ha6S8-2B1000-H1181 rotary encoder which will measure the motor angle and map it to the ankle angle. Then we selected the FX292X-100A-0100-L load transducer which can measure 100 lbf loads and will measure the foot force and map it to our ankle torque. Lastly, we chose to use noninvasive EMG probes that can easily be removed when the prosthetic is taken off.

V. Anatomical Engineering

This system is quite difficult to integrate into the body with a surgical method. One path we considered was osseointegration. This is an advanced reconstructive technique that connects a prosthetic directly to the bone of a residual limb of an amputee. This technique gives direct feedback to and through the skeleton, provides a more natural gait, reduces poor fit issues, allows for greater balance, proprioception, and osseoperception, which is the knowing and feeling where the bones are without looking. In our system, we considered permanently attaching the lever joint of the prosthetic to the desired location on the ankle, as shown in figure 18. Doing this would position the axis of rotation exactly where the body wants it to naturally be. Doing this would simplify the mechanical system, as the motor, gearbox, and the connecting linkage can be adjusted according to the needs of the patient as time progresses. This would lead to the patient having more trust in the process and a more reliable motion. However, this approach comes with many significant drawbacks. Besides the effects of patients not reacting well to the materials used and infections, this procedure would have permanent long-lasting effects, and if the patient gets to a point where they do not need the prosthesis, they would be stuck without an effective ankle joint. Ultimately, this surgical adaptation proves to be too invasive, and too extreme of an approach for this pathology.

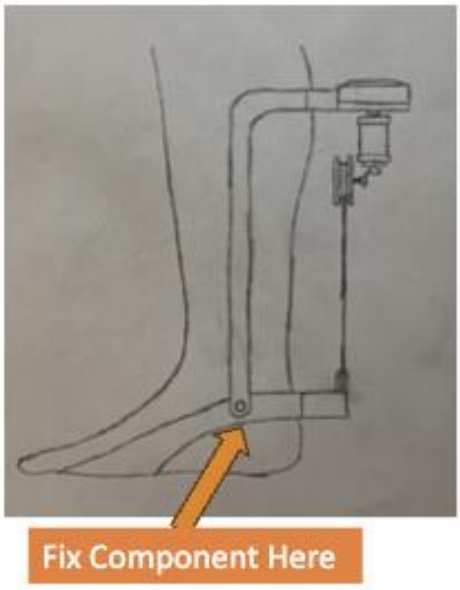

Fig 18: Suggested location to fix prosthesis to ankle